International Journal on Emerging Technologies 11(5): 121-127(2020)
ISSN No. (Print): 0975-8364
ISSN No. (Online): 2249-3255

Red Color Segmentation based Traffic Signs Detection

Manal El Baz[1], Taher Zaki[2] and Hassan Douzi[2]
[1]Ph.D. Student, Image and Pattern Recognition - Intelligent and Communicating Systems Laboratory, Faculty of Sciences, Ibn Zohr University, Agadir, Morocco.
[2]Professor, Image and Pattern Recognition - Intelligent and Communicating Systems Laboratory, Faculty of Sciences, Ibn Zohr University, Agadir, Morocco.

(Corresponding author: Manal El Baz)
(Received 10 June 2020, Revised 13 July 2020, Accepted 01 August 2020)
(Published by Research Trend, Website: www.researchtrend.net)

ABSTRACT: The variety of light and weather conditions makes the detection of traffic signs colors difficult especially in RGB space. In fact, RGB space is dependent of the variation of the illumination caused by the weather or the daytime. Therefore, the normalized RGB is created to avoid the negative effect of the illumination changes. Unfortunately, the ability of the normalized RGB in detecting objects decreases because of losing the contrast. Thus, the variation of the conditions of light and weather and keeping a high detection accuracy represent a challenge in detecting red color of traffic signs. In this paper, the study discusses the detection of the red color of traffic signs under different light and weather conditions: foggy, rainy, sunny and night. In RGB space, we propose a variable threshold that we calculate by using the minimum value and the mean of R channel. However, we use a constant threshold in HSV space. We tested the proposed segmentations in both spaces on images under variety of light and weather conditions. The results obtained proved their efficiency compared with other methods. The two proposed segmentations can detect the red color of traffic signs under the different light and weather conditions while keeping a high accuracy rate.

Keywords: Color detection, HSV space, image processing, red color segmentation, RGB space, traffic signs detection.

Abbreviations: RGB, red green blue; HSV, hue saturation value; IHSL, Improved Hue, Saturation and Luminance; VLWC, variety of light and weather conditions.

I. INTRODUCTION

The detection of traffic signs is an important step in traffic signs detection and recognition system. Indeed, detection results influence on results of recognition step. A traffic sign has two main characteristics: the color and the shape. Thus, Road sign detection can be divided in color-based detection and shape-based detection. Instead, the complexity of the road environment makes the traffic sign detection more difficult. The light variation, the shadow, the reflection and the daytime produce modifications on traffic signs color [1].
There are many researchers worked on detection of the red color of traffic signs using different color spaces such as RGB [2–7] and HSV [8–12] spaces. Wali *et al.,* [2] divide the RGB into three channels R, G and B. They apply the threshold [90, 255] on R channel and [0, 70] on G and B channels. Then they extract the region of interest by doing the logical sum of these filtered channels. Qin *et al.,* [3] use the Euclidean distance to measure the difference between a pixel and the standard red:

$$CD_{red} = \sqrt{((R - 255)^2 + (G - 0)^2 + (B - 0)^2)} \qquad (1)$$

Where CD_{red} is the color distance, R, G and B are the RGB values of a pixel in RGB color space. The lower the CD_{red} value is, the higher is the pixel in the target object. So a pixel is defined as a red pixel if $CD_{red}<TH_{red}$ where TH_{red} is equal to 184 for too dark image, 158 for normal brightness image or 150 for too light image. The normalized RGB color space (ErEgEb) based on chromaticity filter is used by Villalón-Sepúlveda *et al.*, [4] for segmentation. They calculate the mean and the standard deviation of normalized color to determine the thresholding intervals. They consider the interval $[\mu_c - \alpha\sigma_c, \mu_c + \alpha\sigma_c]$ as a threshold for the chromaticity channels E_r and E_g ; where c = E_r, E_g and μ_c is the mean value of the channel c across the ensemble of N_I images. They choose the value 2 for α to guarantee lowest false positive rates. Dutilleux *et al.*, [5] detect the red color in RGB space using the normalization of R channel $\frac{R}{R+G+B}$ to reduce light effects. The authors apply the following threshold:

$$R > \alpha(G + B). \qquad (2)$$

$$R - \max(G, B) > 2\alpha[\max(G, B) - \min(G, B)] \qquad (3)$$

Where $\alpha \in [0.5, 0.75]$. However, Arturo *et al.,* [6] use $\frac{G}{R}$ and $\frac{B}{R}$ to normalize RGB space. The threshold used for segmentation is:

$$g(x, y)= k_1, \text{ if } \begin{cases} R_a \le f_r(x,y) \le R_b \\ TG_a \le \dfrac{f_g(x,y)}{f_r(x,y)} \le TG_b \\ TB_a \le \dfrac{f_b(x,y)}{f_r(x,y)} \le TB_b \end{cases}$$

$$g(x, y)= k_2, \text{ otherwise} \qquad (4)$$

Where $f_r(x, y)$, $f_g(x, y)$ and $f_b(x, y)$ are respectively R, G and B levels of each point of the image. Soheilian *et al.,*

[7] use also the normalized RGB to detect red color. The color threshold used for detection is:

$$\frac{I_r(x,y)}{I_b(x,y)}>T \text{ and } \frac{I_r(x,y)}{I_g(x,y)}>T \quad (5)$$

Where I_r, I_g, I_b are respectively R, G and B channel values. T is the fixed threshold. Bharamgoudar *et al.,* [8] detect red traffic signs by using the HSV color space because it is invariant to illumination changes. Chen *et al.*, [9] use the normalized values of H, S and V as a threshold. The component ranges of red color of road signs used in the threshold are H ≥ 240 or H ≤ 10, S ≥ 40, V ≥ 30. Cao *et al.*, [10] convert the image to HSV space and calculate the means and the standard deviations of H and S. After multiple test experiments, they determine the threshold ranges for every channel: H > 0.90 or H < 0.10, S > 0.40, V > 0.35. Chandiramani *et al.*, [11] define threshold values for HSV components by the method of analysis on signs segmented manually under different weather and illumination conditions. Youssef *et al.*, [13] use the Improved Hue, Saturation and Luminance IHSL color space to detect road signs under variation of light condition. Thus, they apply the following operation to convert the image from RGB to IHSL:

$$\mathrm{IHSL}(x,y)=\begin{cases}0, \text{ if } \max\left(I_R(x,y), I_G(x,y), I_B(x,y)\right)=I_G(x,y)\vee \\ \left(\left|I_R(x,y)-I_G(x,y)\right|<\zeta\wedge\left|I_B(x,y)-I_G(x,y)\right|<\gamma\right) \\ F_{IHSL}\left(I_R(x,y), I_G(x,y), I_B(x,y)\right), \text{ otherwise}\end{cases} \quad (6)$$

Where IHSL(x, y) is the IHSL color space value for the pixel in position (x, y), that have I_R , I_G , I_B RGB values, F_{ihsl} is the usual conversion from RGB color space to IHSL color space and ζ , γ thresholds that are set based on lighting conditions. They use the maximum of the distribution of each RGB color channel ε_n to detect the lighting condition and to adopt the values of ζ and γ. Then they use the normalized Hue-Saturation method and post processing steps to find the potential pixels belonging to traffic signs. HSI is the chosen colour space by de la Escalera *et al.,* [14]. To avoid lighting condition, they only take H and S in account:

$$H(i)=\begin{cases}255\,\frac{i_{min} i}{i_{min}}, 0\le i\le i_{min} \\ 0, i_{min}<i<i_{max} \\ 255\,\frac{i i_{max}}{i_{max}},\ i_{max}\le i\le 255\end{cases} \quad (7)$$

$$S(i)=\begin{cases}i,\ 0\le i\le i_{min} \\ 255,\ i_{min}\le i\le 255\end{cases} \quad (8)$$

Nevertheless, although these methods perform well in detecting traffic signs color, they present some limits. Variant lighting conditions and illumination of traffic signs affect the performance of the detection in [2]. Moreover, threshold value is not dynamically selected in [3] and it depends on the large number of images in special environment.

In this paper, we focus on segmentation of red color of traffic signs in both RGB and HSV spaces under different light and weather conditions: foggy, rainy, sunny and night. For RGB segmentation, we propose a variable threshold in which we calculate the mean and the min of red color pixels to determine intervals of the threshold. Conversely, we propose a constant threshold for HSV segmentation. Results of proposed segmentations show their efficiency compared with the state of the art methods. This paper is organized as follows: We present the method used in RGB segmentation and the segmentation in HSV in Section II. We discuss the results of the two segmentations in Section III and we conclude this work in Section IV.

II. MATERIALS AND METHODS

A. Segmentation in RGB

The proposed segmentation of red color in RGB space follows these steps: firstly, we resize the image to 200 × 200 then we do the normalization by applying the $\frac{R}{G}$, $\frac{R}{B}$ and $\frac{R}{R+G+B}$. Finally, we apply the threshold that is determined by using the min and the mean of $\frac{R}{G}$, $\frac{R}{B}$ and $\frac{R}{R+G+B}$.

Fig. 1. Framework of the segmentation in RGB.

We normalize the RGB by using the following formulation in order to reduce the lighting effects:

$$\frac{R}{G}, \frac{R}{B}, \frac{R}{R+G+B}. \quad (9)$$

After the normalization of RGB space, we calculate the mean and the variance of respectively $\frac{R}{G}$, $\frac{R}{B}$ and $\frac{R}{R+G+B}$ by using the following formulation:

$$\mu_{\frac{R}{G}}=\frac{\Sigma\left(I_{\frac{R}{G}}\times f_{I_{\frac{R}{G}}}\right)}{N_{\frac{R}{G}}}. \quad (10)$$

$$\sigma^2_{\frac{R}{G}}=\frac{\Sigma\left(\left(I_{\frac{R}{G}}-\mu_{\frac{R}{G}}\right)^2\times f_{I_{\frac{R}{G}}}\right)}{N_{\frac{R}{G}}}. \quad (11)$$

$$\mu_{\frac{R}{B}}=\frac{\Sigma\left(I_{\frac{R}{B}}\times f_{I_{\frac{R}{B}}}\right)}{N_{\frac{R}{B}}}. \quad (12)$$

$$\sigma^2_{\frac{R}{B}}=\frac{\Sigma\left(\left(I_{\frac{R}{B}}-\mu_{\frac{R}{B}}\right)^2\times f_{I_{\frac{R}{B}}}\right)}{N_{\frac{R}{B}}}. \quad (13)$$

$$\mu_{\frac{R}{R+G+B}}=\frac{\Sigma\left(I_{\frac{R}{R+G+B}}\times f_{I_{\frac{R}{R+G+B}}}\right)}{N_{\frac{R}{R+G+B}}}. \quad (14)$$

$$\sigma^2_{\frac{R}{R+G+B}}=\frac{\Sigma\left(\left(I_{\frac{R}{R+G+B}}-\mu_{\frac{R}{R+G+B}}\right)^2\times f_{I_{\frac{R}{R+B+G}}}\right)}{N_{\frac{R}{R+G+B}}}. \quad (15)$$

where

$I_{\frac{R}{G}}$, $I_{\frac{R}{B}}$ and $I_{\frac{R}{R+G+B}}$ are respectively the value of $\frac{R}{G}$, $\frac{R}{B}$ and $\frac{R}{R+G+B}$;

$f_{I_{\frac{R}{G}}}$, $f_{I_{\frac{R}{B}}}$ and $f_{I_{\frac{R}{R+G+B}}}$ are respectively the number of pixels with color value $I_{\frac{R}{G}}$, $I_{\frac{R}{B}}$ and $I_{\frac{R}{R+G+B}}$;

$N_{\frac{R}{G}}$, $N_{\frac{R}{B}}$ and $N_{\frac{R}{R+G+B}}$ are respectively the total number of pixels of $I_{\frac{R}{G}}$, $I_{\frac{R}{B}}$ and $I_{\frac{R}{R+G+B}}$;

$\mu_{\frac{R}{G}}$, $\mu_{\frac{R}{B}}$ and $\mu_{\frac{R}{R+G+B}}$ are respectively the mean of $I_{\frac{R}{G}}$, $I_{\frac{R}{B}}$ and $I_{\frac{R}{R+G+B}}$;

$\sigma^2_{\frac{R}{G}}$, $\sigma^2_{\frac{R}{B}}$ and $\sigma^2_{\frac{R}{R+G+B}}$ are respectively the variance of $I_{\frac{R}{G}}$, $I_{\frac{R}{B}}$ and $I_{\frac{R}{R+G+B}}$.

In statistics, the empirical rule [15]is divided in three parts:

— $\mu\pm\sigma$contains 68% of data set;

— $\mu\pm 2\sigma$contains 95% of data set;

— $\mu\pm 3\sigma$ contains 99.7% of data set.

According to the empirical rule, we consider:

$$min_{\frac{R}{G}} = \mu_{\frac{R}{G}} - \alpha\sigma_{\frac{R}{G}}. \quad (16)$$

$$min_{\frac{R}{B}} = \mu_{\frac{R}{B}} - \alpha\sigma_{\frac{R}{B}}. \quad (17)$$

$$min_{\frac{R}{R+G+B}} = \mu_{\frac{R}{R+G+B}} - \alpha\sigma_{\frac{R}{R+G+B}}. \quad (18)$$

Where $min_{\frac{R}{G}}$, $min_{\frac{R}{B}}$ and $min_{\frac{R}{R+G+B}}$ are respectively the minimum value of $I_{\frac{R}{G}}$, $I_{\frac{R}{B}}$ and $I_{\frac{R}{R+G+B}}$;

α a constant that is equal to 1, 2 or 3.

We tested the three values of α (α=3, α=2 and α=1) in the segmentation and we got the result shown in Fig. 2.

As viewed in Fig. 2, α = 1 is the best value for this segmentation. It eliminates elements of the background that are not red.

In some images; in which the min value is superior than 176; the segmentation does not include some red pixels like in Fig. 3(b). For that reason, we apply the threshold [| min – 40 |, 255] if $min\geq 176$ and we get the result shown in Fig. 3(c). Thus, we use the following threshold for R channel:

$$\begin{cases} I_R \in \left(\left[\left|min_{\frac{R}{G}}-40\right|,255\right] \cup \left[\left|min_{\frac{R}{R+G+B}}-40\right|,255\right]\right) \\ \cap \left[\left|min_{\frac{R}{B}}-40\right|,255\right], \text{ if } min_{\frac{R}{G}}, min_{\frac{R}{B}}, min_{\frac{R}{R+G+B}} \in [176,255] \\ I_R \in \left(\left[\left|min_{\frac{R}{G}}\right|,255\right] \cup \left[\left|min_{\frac{R}{R+G+B}}\right|,255\right]\right) \\ \cap \left[\left|min_{\frac{R}{B}}\right|, 255\right], \text{ otherwise} \end{cases} \quad (19)$$

where

$$min_{\frac{R}{G}} = \mu_{\frac{R}{G}} - \sigma_{\frac{R}{G}}. \quad (20)$$

$$min_{\frac{R}{B}} = \mu_{\frac{R}{B}} - \sigma_{\frac{R}{B}}. \quad (21)$$

$$min_{\frac{R}{R+G+B}} = \mu_{\frac{R}{R+G+B}} - \sigma_{\frac{R}{R+G+B}} \quad (22)$$

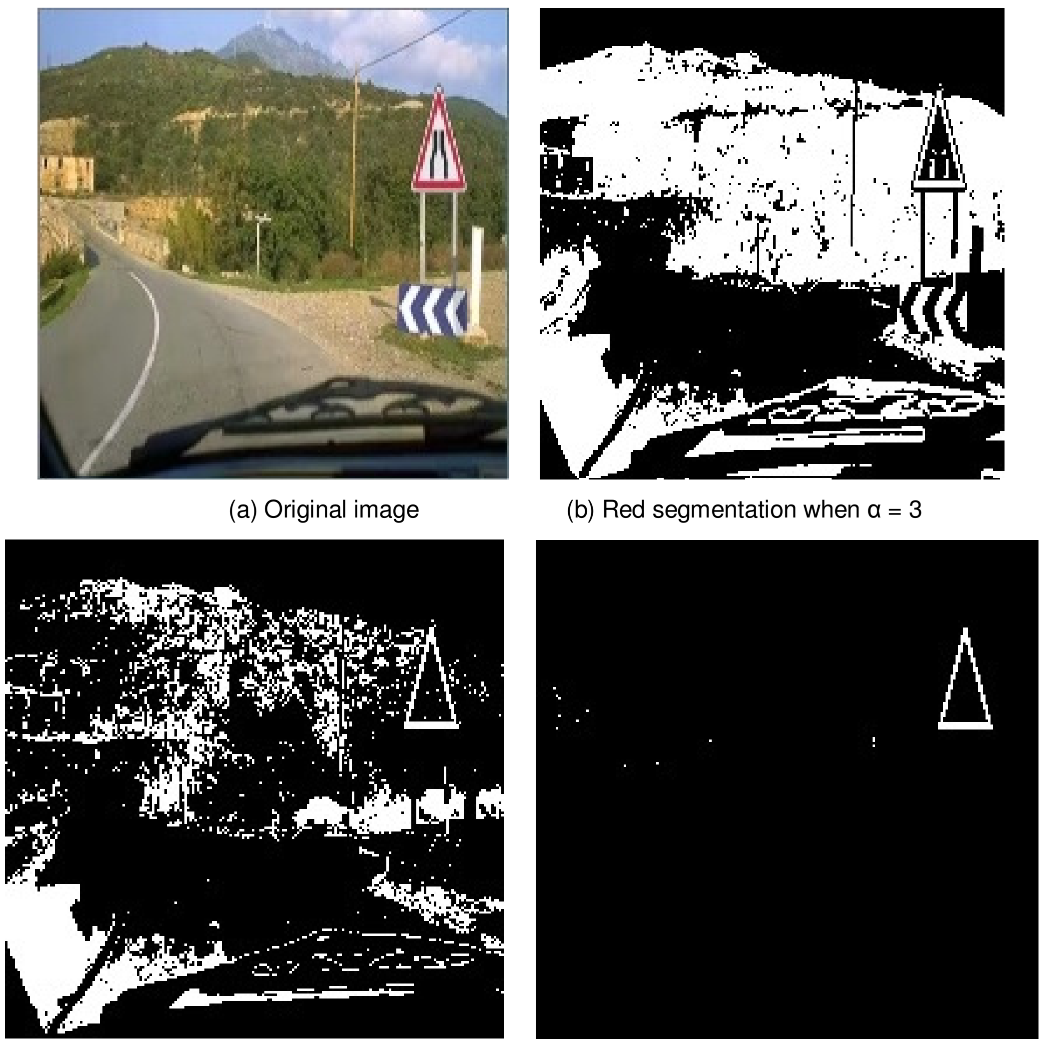

(a) Original image (b) Red segmentation when α = 3

(c) Red segmentation when α = 2 (d) Red segmentation when α = 1

Fig. 2. Red color detection.

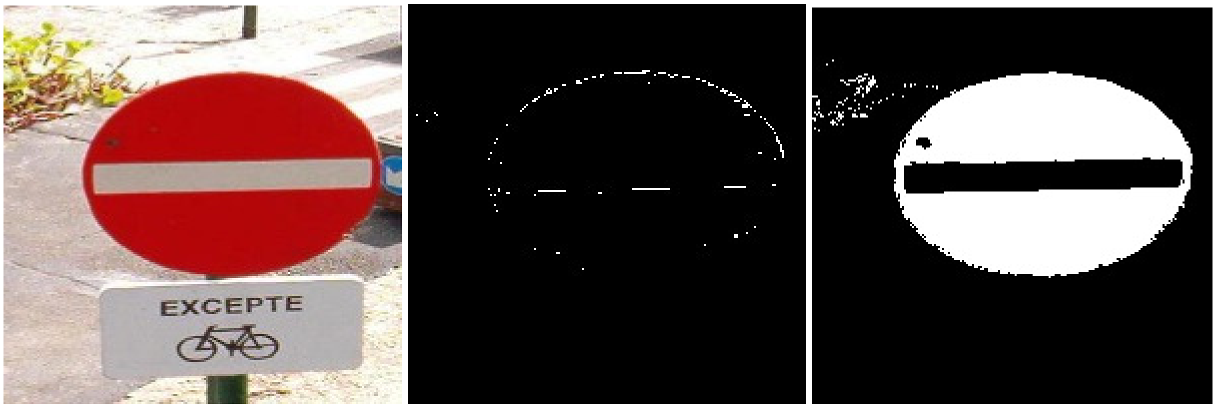

(a) Original image (b) For the threshold [|min|, 255] (c) For the threshold [|min – 40|, 255]

Fig. 3. Red color segmentation when the $\min \geq 176$.

The RGB codes of red color degradation are defined in Table 1.

Table 1: RGB codes of red color degradation.

Color	RGB code
	(255,0,0)
	(128,0,0)
	(139,0,0)
	(178,34,34)
	(220,20,60)
	(255,99,71)
	(240,128,128)
	(250,128,114)
	(255,69,0)
	(255,153,128)

According to Table 1, we note that R channel values are superiors than G channel values and B channel values for red color degradation.

$$\begin{cases} I_R \geq 1.66 I_G \\ I_R \geq 2 I_B \end{cases} \quad (23)$$

For that reason, we consider this threshold for G and B channel:

$$I_G \in \left(\left[0, \mu_{\frac{R}{G}}\right] \cup \left[0, \mu_{\frac{R}{R+G+B}}\right] \right) \cap \left[0, \frac{\mu_{\frac{R}{B}}}{1.66}\right] \quad (24)$$

$$I_B \in \left(\left[0, \frac{\mu_{\frac{R}{G}}}{2}\right] \cup \left[0, \mu_{\frac{R}{R+G+B}}\right] \right) \cap \left[0, \mu_{\frac{R}{B}}\right] \quad (25)$$

B. Segmentation in HSV

We convert the resized image (200×200) from RGB to HSV space. Then we segment the image by using the following threshold:

$$h \in [0,10] \cup [160,255] \quad (26)$$

$$s \in [150,255] \quad (27)$$

$$v \in [0,255] \quad (28)$$

Fig. 4. Framework of the segmentation in HSV.

III. RESULTS AND DISCUSSION

We tested the methods on 111 images that contain red traffic signs under variety of light and weather conditions (VLWC): foggy, rainy, sunny and night. We compared proposed red segmentations with Wali *et al.,* [2] method, Chen *et al.*, [9] method, Cao *et al.*, [10] method and Koresh [16] method. Wali *et al.,* [2] apply the threshold [90, 255] on R channel and [0, 70] on G and B channels to detect the red color in the image. However, Chen *et al.,* [9] detect red traffic signs by using the HSV color space. They apply the threshold: $H \geq 240$ or $H \leq 10$, $S \geq 40$, $V \geq 30$. Cao *et al.*, [10] use also HSV space for segmentation. They calculate the means and the standard deviations of H and S. After multiple test experiments, they choose the threshold ranges: $H > 0.90$ or $H < 0.10$, $S > 0.40$, $V > 0.35$. Koresh [16] applies the segmentation in HSV space. He uses the threshold ranges: $S<0.2$ and $0<H<10$, $320<H<360$. To measure the performance of those methods, we use the following metrics:

$$\text{Precision} = \frac{TP}{TP+FP} \quad (29)$$

$$\text{Recall} = \frac{TP}{TP+FN} \quad (30)$$

$$F\text{-score}= 2\times\frac{\text{Precision} \times \text{Recall}}{\text{Precision}+\text{Recall}} \quad (31)$$

where

— True Positive TP: number of red traffic signs that are detected as red signs.

— False Positive FP: a non-red sign that is detected as a red traffic sign.

— False Negative FN: a red traffic sign that is detected as a non-red sign.

Table 2 shows results of detecting red color of traffic signs in RGB and HSV spaces for the six methods.

Table 2: Results of the segmentation in RGB and HSV color space.

	Precision%	Recall%	F-score%
Our RGB segmentation	**93.49**	**88.27**	**90.80**
Our HSV segmentation	79.50	71.51	75.29
Wali's RGB segmentation [2]	82.86	64.80	72.73
Chen's HSV segmentation [9]	81.05	69.27	74.70
Cao's HSV segmentation [10]	61.54	67.04	64.17
Koresh's HSV segmentation [16]	61,79	73,18	67,01

As shown in Table 2, the proposed RGB segmentation has the highest precision, recall and F-score rates compared with the other methods. Moreover, the proposed HSV segmentation obtains recall and F-score rates superiors than rates of Wali *et al.*, [2] method, Chen et al. [9] method and Cao *et al.*, [10] method. However, its result in term of precision is lower than Wali *et al.*, [2] method and Chen *et al.*, [9] method, also its results in term of recall is lower than the one of Koresh [16] method. Accordingly, results demonstrate that the performance of segmentation of red color using the variable threshold is better than the fixed one. In fact, the variable threshold allows the algorithm to adopt the segmentation for each image.

To know how the methods behave in each light and weather conditions, Fig. 5 illustrates results of the methods in foggy, rainy, night and sunny conditions. The proposed RGB segmentation gives the best results. It can detect accurately the red color of traffic signs whatever the illumination and weather conditions. Wali *et al.,* [2] segmentation performs well in rainy and night conditions but it fails to detect red traffic signs in foggy and sunny conditions. The proposed HSV segmentation shows false alarm at night in detecting some black pixels. Similarly, Chen *et al.,* [9], Cao *et al.*, [10] and Koresh [16] methods segment part of the background. Chen *et al.,* [9] thresholding segments the top part of the image of night condition and Cao *et al.,* [10] method detects the road as a red region. Moreover, Koresh [16] method detects the gray part and some regions in the top part of the image.

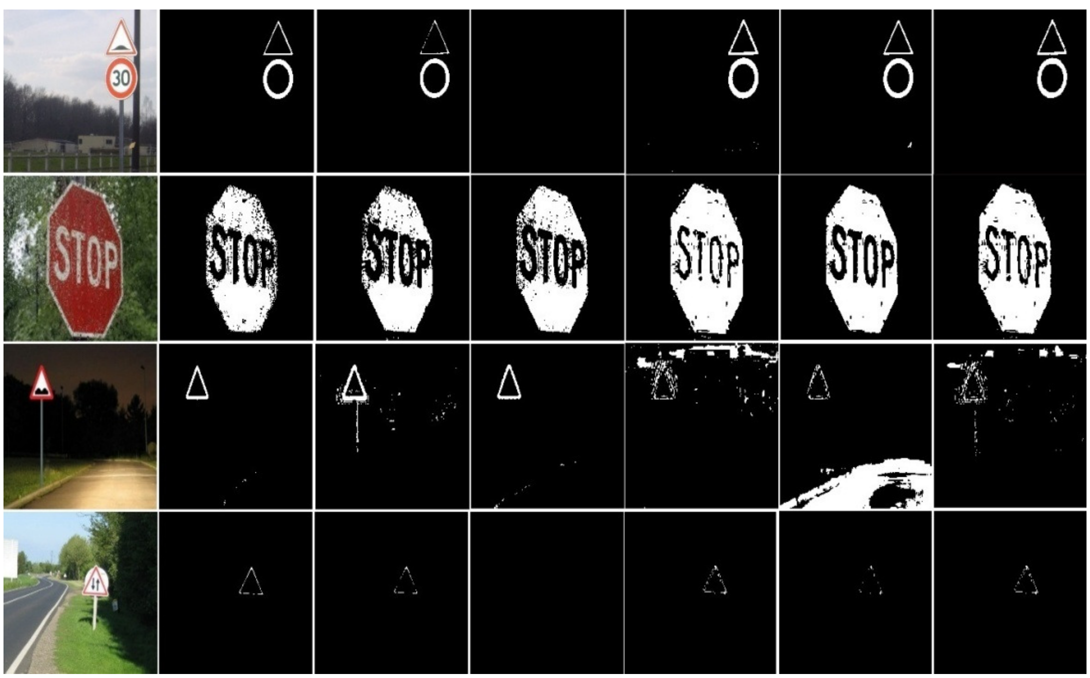

Fig. 5. Comparison of the methods under VLWC. From left to right: original image, propose d RGB segmentation, proposed HSV segmentation, Wali's RGB segmentation [2], Chen's HSV segmentation [9], Cao's HSV segmentation [10], Koresh's HSV segmentation [16]. From top to bottom: foggy, rainy, night, sunny.

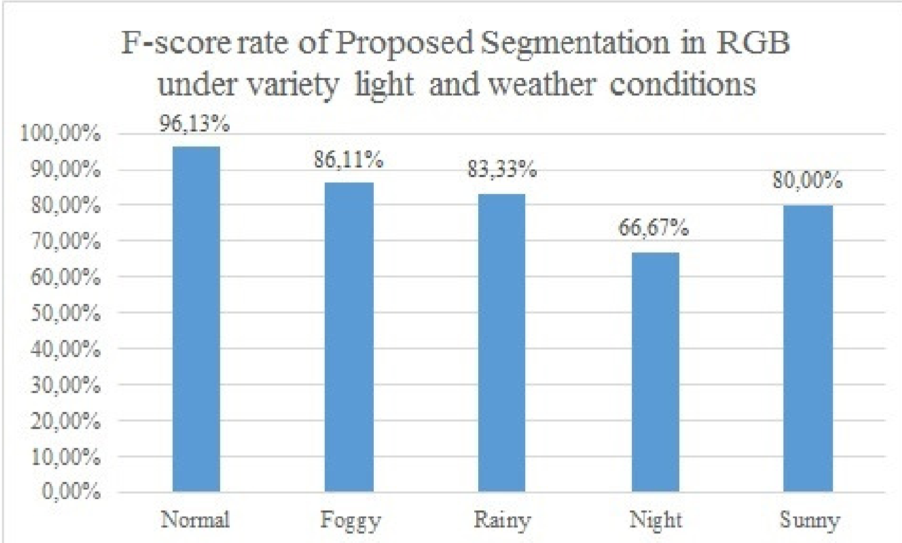

Fig. 6. F-score rate of proposed segmentation in RGB under VLWC.

The F-score rate obtained for the proposed RGB segmentation in each light and weather conditions is depicted in Fig. 6.
According to Fig. 6, we notice that the proposed red segmentation in RGB space has good results in normal, foggy, rainy and sunny conditions. However, its performance at night is lower than other light conditions. In fact, the false positive rate increases at night.

IV. CONCLUSION

We have presented the segmentation in both RGB and HSV spaces. We proposed a variable threshold for RGB space to detect red color of road signs. We determine the threshold by using the minimum value and the mean of R channel. In contrast, we proposed a constant threshold for HSV space. We tested the methods on 111 images that contain red traffic signs under variety of light and weather conditions. We compared the proposed segmentations with state of the art methods and they perform accurately under foggy, sunny, rainy and night conditions. The proposed variable threshold in RGB space shows 90.80% however, we obtain 75.29% for the constant threshold in HSV space. Results show that the segmentation of red color of traffic signs using the variable threshold is better than the fixed one. In contrast, the proposed segmentation in RGB has a lower performance rate at night compared with the other light conditions.

V. FUTURE SCOPE

The proposed segmentation in RGB space has a lower performance at night compared with the other light and weather conditions because of false positives. Moreover, the proposed segmentation in HSV space shows also false positives in detecting some black pixels at night. In future work, we will focus on decreasing the rate of false positive detection at night for the two methods.

Conflict of Interest. This article has no conflict of interest.

ACKNOWLEDGEMENT

This work is supported by Image and Pattern Recognition - Intelligent and Communicating Systems Laboratory, Faculty of Sciences of Agadir.

REFERENCES

[1]. Foucher, P. (2010). Détection et Reconnaissance de la Signalisation Verticale par Analyse d'Images. *Laboratoire Central des Ponts et Chaussées, Paris, France,* pp. 9. (In French)

[2]. Wali, S. B., Hannan, M. A., Abdullah, S.,Hussain, A. and Samad, S. A. (2015). Shape Matching and Color Segmentation based Traffic Sign Detection System. *Przegląd Elektrotechniczny, 1*(1): 38–42.doi: 10.15199/48.2015.01.06

[3]. Qin, F., Fang, B., and Zhao, H. (2010). Traffic Sign Segmentation and Recognition in Scene Images. *In: 2010 Chinese Conference on Pattern Recognition: Chongqing, China*, 1–5.

[4]. Villalón-Sepúlveda, G., Torres-Torriti, M., and Flores-Calero, M. (2017). Traffic Sign Detection System for Locating Road Intersections and Roundabouts: The Chilean Case. *Sensors*, *17*(6): 1207. doi: 10.3390/s17061207

[5]. Dutilleux, G., and Charbonnier, P. (2005). Détection de Signalisation Routière pour Ajustement de Formes Prototypes. *20 Colloque sur le Traitement du Signal et des Images,* 488–491. (In French)

[6]. De la Escalera, A., Moreno, L. E., Salichs, M. A., and Armingol, J. M. (1997). Road Traffic Sign Detection and Classification. IEEE Transactions on Industrial Electronics, *6*(4): 848-859.doi: 10.1109/41.649946

[7]. Soheilian, B., Arlicot, A., and Paparodits, N. (2010). Extraction de Panneaux de Signalisation Routière dans des Images Couleurs.*In : Actes du 17ème Congrès Francophone en Reconnaissance de Formes et Intelligence Artificielle, RFIA'10 ; Caen, France,* 743–750. (In French)

[8]. Bharamgoudar, S.R., and Kale, K. A. (2014). Traffic sign detection using mathematical morphology.

International Journal of Advances in Science Engineering and Technology, *2*: 26–29.doi: IJASEAT-IRAJ-DOI-1343
[9]. Chen, Y., Xie, Y., and Wang, Y. (2013). Detection and recognition of traffic signs based on HSV vision model and shapefeatures.*Journal of Computers*, *8*(5):1366–1370. doi: 10.4304/jcp.8.5.1366-1370
[10]. Cao, J., Song, C., Peng, S., Xiao, F. and Song, S. (2019). Improved traffic sign detection and recognition algorithm for intelligent vehicles. *Sensors (Basel), 19*(18): 4021. doi: 10.3390/s19184021
[11]. Chandiramani, G.,and Dhotre, M. R. (2015). Vision Based Road Sign Detection and Recognition. *International Journal of Scientific Engineering and Research, 3*: 43–47.
[12]. Horak, K., Cip, P., and Davidek, D. (2016). Automatic Traffic Sign Detection and Recognition Using Colour Segmentation and Shape Identification. *MATEC Web of Conferences, 68*: 17002. doi: 10.1051/matecconf/20166817002
[13]. Youssef, A., Albani, D., Nardi, D., and Bloisi, D. D. (2016). Fast traffic sign recognition using color segmentation and deep convolutional networks.*In: International Conference on Advanced Concepts for Intelligent Vision Systems; Lecce, Italy*, 205-116.
[14]. De la Escalera, A., Armingol, J. M., and Mata, M. (2003). Traffic sign recognition and analysis for intelligent vehicles. *Image and Vision Computing*, *21*(3): 247–258. doi : 10.1016/S0262-8856(02)00156-7
[15]. Shafer, D. S., and Zhang, Z. (2012). Beginning Statistics(v. 1.0). pp. 92.
[16]. Koresh, H. J. D. (2019). Computer vision based traffic sign sensing for smart transport. *Journal of Innovative Image Processing*, *1*(1): 11–19. doi: 1036548/jiip.2019.1.002

How to cite this article: El Baz, M., Zaki, T. and Douzi, H. (2020). Red Color Segmentation based Traffic Signs Detection. *International Journal on Emerging Technologies, 11*(5): 121–127.